

A Performance Analysis of BFT Consensus for Blockchains

J.D. CHAN, Y.C. TAY, and BRIAN R.Z. YEN, National University of Singapore, Singapore

Distributed ledgers are common in the industry. Some of them can use blockchains as their underlying infrastructure. A blockchain requires participants to agree on its contents. This can be achieved via a consensus protocol, and several BFT (Byzantine Fault Tolerant) protocols have been proposed for this purpose. How do these protocols differ in performance? And how is this difference affected by the communication network? Moreover, such a protocol would need a timer to ensure progress, but how should the timer be set?

This paper presents an analytical model to address these and related issues in the case of crash faults. Specifically, it focuses on two consensus protocols (Istanbul BFT and HotStuff) and two network topologies (Folded-Clos and Dragonfly). The model provides closed-form expressions for analyzing how the timer value and number of participants, faults and switches affect the consensus time. The formulas and analyses are validated with simulations. The conclusion offers some tips for analytical modeling of such protocols.

CCS Concepts: • **Networks** → **Network protocols; Application layer protocols**; • **Computing methodologies** → **Modeling methodologies; Distributed algorithms**.

Additional Key Words and Phrases: Byzantine faults, consensus protocols, blockchain, performance model

ACM Reference Format:

J.D. Chan, Y.C. Tay, and Brian R.Z. Yen. 2018. A Performance Analysis of BFT Consensus for Blockchains. 1, 1 (November 2018), 20 pages. <https://doi.org/XXXXXXXX.XXXXXXX>

1 INTRODUCTION

There is considerable current interest in the use of blockchains to implement distributed ledgers for finance, health care, energy, logistics, etc. [11]. This requires continual consensus among interested parties in the system. Research on consensus protocols is mostly split between proof-based consensus (like Bitcoin) and vote-based consensus [30].

A vote-based protocol for enforcing consensus must guard against errant (possibly malicious) validator behavior. It is said to be *Byzantine Fault Tolerant* (BFT) if it can achieve consensus despite arbitrary misbehavior. There is a large variety of BFT protocols. They differ in terms of failure models, delay assumptions, cryptographic requirements, etc. Much of the impetus in developing new protocols lies in pushing their performance.

The performance of these protocols are measured via complexity analysis (e.g. number of messages or rounds), in empirical or simulation experiments, or with analytical models. Despite decades of such analysis of BFT consensus, much remains unknown regarding their behavior.

For example, to ensure the protocol progresses despite failures, a common technique lies in setting a *timer*; when it expires, the protocol assumes there is a fault, and restarts the consensus process. This timer has some initial value τ_0 , but the value is usually increased upon timer expiry. How should τ_0 be set?

Authors' Contact Information: J.D. Chan; Y.C. Tay, dcstayyc@nus.edu.sg; Brian R.Z. Yen, National University of Singapore, Singapore.

Permission to make digital or hard copies of all or part of this work for personal or classroom use is granted without fee provided that copies are not made or distributed for profit or commercial advantage and that copies bear this notice and the full citation on the first page. Copyrights for components of this work owned by others than the author(s) must be honored. Abstracting with credit is permitted. To copy otherwise, or republish, to post on servers or to redistribute to lists, requires prior specific permission and/or a fee. Request permissions from permissions@acm.org.

© 2018 Copyright held by the owner/author(s). Publication rights licensed to ACM.

ACM XXXX-XXXX/2018/11-ART

<https://doi.org/XXXXXXXX.XXXXXXX>

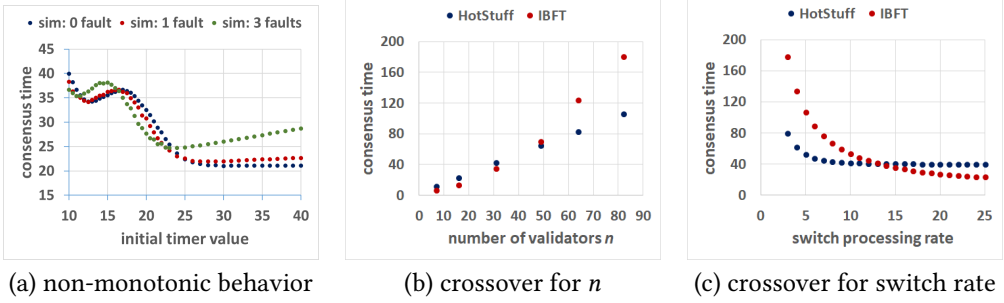


Fig. 1. Simulated consensus time for (a) HotStuff with varying number of faults ($n = 16$, clique), (b) HotStuff vs IBFT on Dragonfly ($v_d = 5$, $r_s^P = 9$) and (c) HotStuff vs IBFT on Dragonfly ($v_d = 3$, $n = 31$). The unit of time on the vertical axis follows that for message processing time at a validator (see Sec. 3.4).

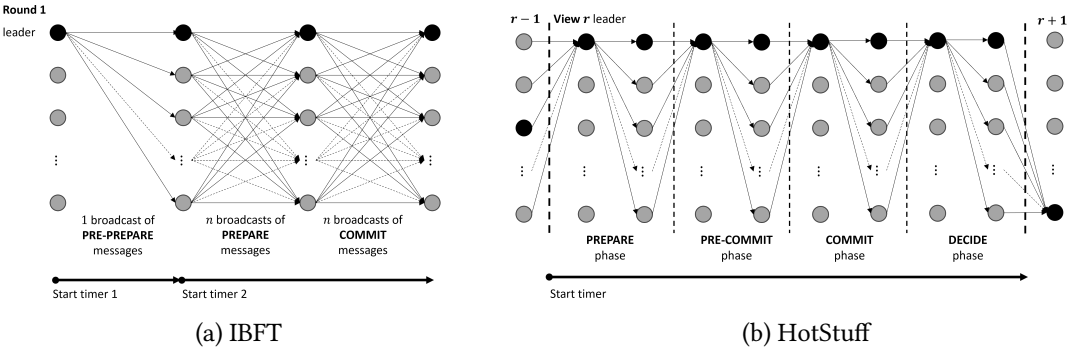


Fig. 2. IBFT and HotStuff have very different patterns for message exchange.

For guidance, we simulated HotStuff [31], a well-known BFT protocol for blockchains, and measured the time T to gather consensus for a block. Fig. 1(a) shows how T varies with τ_0 and the number of faults. How can one analytically describe this interesting, non-monotonic behavior?

In the simulations for Fig. 1(a), we factor out the impact of the network connecting the nodes by using 0 message delay between any two nodes. What if the network delays are not negligible? How might two topologies differ in their impact on T ?

A network can affect T through congestion delays. We therefore expect that the same topology can have different impact on two protocols, if their message patterns differ. For example, consider the pattern in Fig. 2(a) for IBFT (Istanbul BFT) protocol [20], which is very different from the one in Fig. 2(b) for HotStuff. One may expect that, for the same topology, congestion delays can have greater impact on IBFT than HotStuff.

However, simulation results in Fig. 1(b) show that, for the Dragonfly [25], IBFT can be faster or slower than HotStuff, depending on the number of participants. Fig. 1(c) shows a similar slower/faster crossover depending on how fast a switch or router can process a message. How do the protocol and topology parameters determine the crossover point in their consensus time?

This paper presents three contributions: (1) An analysis of how BFT consensus time depends on the number of validators and faults, timer value and network topology. (2) A comparison of two protocols' performance, and two topologies' impact. (3) An approach to analytic modeling of consensus protocols.

Below, we begin with a review of related work in Sec. 2. Sec. 3 introduces necessary definitions and notation, and describes two protocols (IBFT and HotStuff) and two topologies (Dragonfly and Folded-Clos) that we use for analyzing consensus time; it also presents the approach to the performance analysis and its validation. A Byzantine validator can cause arbitrary performance degradation [8], so we only consider crash faults. The performance model is presented in Sec. 4 for cliques and Sec. 5 for non-clique topologies. Sec. 6 highlights some conclusions about the consensus time for HotStuff and IBFT, and the modeling approach.

2 RELATED WORK

BFT protocols were introduced 40-odd years ago [23]. The problem formulation helped to kick-start research on distributed computing, and many variations followed thereafter. The PBFT (Practical BFT) protocol [7] revived interest in the problem, and this was further boosted by the application of BFT consensus to blockchains [30]. IBFT and HotStuff are examples of BFT protocols that are specifically designed for blockchains [6, 20].

Pre-PBFT, the design of BFT protocols was mostly driven by changes in assumptions (e.g. network synchrony or failure detectors) and improvements in complexity (e.g. number of rounds or bits). However, the performance of a protocol goes beyond algorithmic complexity. Experimental measurements show that consensus latency and throughput can be significantly affected by message size, verification algorithm, network topology, attack model, etc. [3, 12, 13, 26].

In any experimental study, measurements are only done for some particular choice and combination of values for the variables (e.g. number of switches) or parameters (e.g. timer value), so the observations may not be conclusive. For example, one protocol may be faster than another in some observed part of the parameter space, but not in some other, unobserved part.

One could get a global view of the parameter space by using an analytical model of the protocol. Unfortunately, we could not find an adequate model in the literature. For example, Ricci et al. model the delays experienced by clients who submit transactions that make up the blocks, but they do not model the consensus protocol [24], and Ni et al.'s model for blockchains in a 6G context does not include the timer [22].

In terms of modeling technique, an obvious choice would be Markov chains [16], but such models rarely yield closed-form expressions that provide a global view; one ends up solving them numerically for some choice of parameter values so, again, we can only see parts of the parameter space. The same is true of queueing and Petri net models [18, 32].

In contrast, we present a modeling approach that is based on crude approximations and elementary probabilistic arguments. It also uses bottleneck analysis, which is simple, yet effective, as demonstrated by the impactful Roofline model [28]. This approach leads to closed-form expressions that facilitate performance analysis of consensus protocols on realistic network topologies.

3 PRELIMINARIES

We are interested in how the performance of BFT consensus depends on the protocol and the network topology. Below, Sec. 3.1 first describes two BFT protocols, and Sec. 3.2 follows with two topologies. Sec. 3.3 then states the key equation for estimating consensus time, taking faults into account. Sec. 3.4 describes the simulator that we use to validate the performance model. The reader can skip forward to Sec. 4 and Sec. 5, and refer to this section (or Table 1 in the Appendix) for definitions and notation when needed.

3.1 BFT Protocols

We want to know how consensus time depends on the number of validators n . We therefore consider a *closed system*, where n is fixed; there are standard techniques for using a closed system as a

submodel for an *open system* [27], where n varies as validators come and go. Let n_f denote the number of faulty validators, and $n_w = n - n_f$ the number of nonfaulty or *working* validators.

The correctness of BFT protocols depends critically on their assumptions regarding message delays [19]. We therefore pick two protocols with the same assumption, namely partial synchrony [10]. IBFT and HotStuff are chosen because they have canonical but very different patterns for message exchange (see Fig. 2).

These 2 protocols specify a bound $f \geq n_f$, and are provably correct if $n \geq 3f + 1$. A *quorum* consists of $2f + 1$ valid votes for a consensus.

3.1.1 Terminology and Notation (Protocols).

Each protocol is run by n validators or *nodes*. A *block* is a collection of data (client or ledger information, etc.). A *blockchain* is a sequence of blocks. Each validator adds blocks to its own copy of the blockchain, and the essence of the consensus lies in ensuring all copies are the same.

The j th *consensus instance* is the state in which the $(j - 1)$ th block is in the blockchain and the validators are working out the consensus for adding the j th block.

A *round* (in IBFT) or *view* (in HotStuff) is a single iteration of the protocol for a consensus instance. Each successful completion of 1 round implies consensus. Each round aims to garner validator consensus for adding a block to the blockchain. Unless there are timeouts, a fault-free run of the protocol would lead to consensus in 1 round.

Each validator has a *timer*; if it does not reach consensus upon timer expiry, it will initiate a *round change*. Faults and timeouts can cause multiple round changes before consensus is reached. It is possible for multiple validators to undergo round change while others have already reached consensus. Crucially, a *full round change* refers to the case where all validators undergo round change for the same round. This can happen if the leader crashes, or validators time out. The initial value for a timer is τ_0 . The value is doubled everytime the timer expires (i.e. exponential backoff).

We now describe the two protocols, focusing on the message exchange and omitting details for verification, encryption, etc.

3.1.2 IBFT Consensus Protocol.

IBFT is an adaptation of PBFT for the Quorum blockchain [20]. A round has a single validator that is a *leader*; this role is rotated among validators. Conceptually, a round has 3 phases (see Fig. 2(a)):

(PRE-PREPARE) In the PRE-PREPARE phase, the leader starts its first timer (see Fig. 2(a)) and broadcasts a PRE-PREPARE to all validators. Upon receiving a PRE-PREPARE, a validator starts its second timer, transitions to the PREPARE phase, and broadcasts a PREPARE to all validators.

(PREPARE) While in the PREPARE phase, a validator that receives a quorum of $2f + 1$ PREPARE messages transitions into the COMMIT phase and broadcasts a COMMIT message.

(COMMIT) A validator that receives a quorum of COMMIT messages considers that as indicating consensus; adds the block to its blockchain, starts its first timer and returns to the PRE-PREPARE phase for the next consensus instance.

If a validator's timer expires before consensus is reached, it initiates a separate round change protocol by broadcasting a ROUND-CHANGE message: upon receiving a quorum of these messages, the new leader broadcasts a PRE-PREPARE message and the protocol resumes.

If the (pre-determined) leader for the next round receives a quorum of ROUND-CHANGE messages, it abandons the current round, doubles its timer duration, enters a PRE-PREPARE phase, and starts a fresh round for the block.

3.1.3 HotStuff Consensus Protocol.

HotStuff is used as a basis for blockchain protocols like LibraBFT for the Diem blockchain [6]. A *view* in HotStuff is like a round in IBFT, so we use the two terms interchangeably. As in IBFT, each

view has a *timer*, and a *leader* that is also a validator. A leader is randomly chosen as views change. A view has 4 phases (see Fig. 2(b)):

- (PREPARE) In the PREPARE phase, a validator starts its timer and sends a NEW-VIEW message to the leader. Upon receiving $2f + 1$ NEW-VIEW messages, the leader broadcasts a PREPARE message.
- (PRECOMMIT) Upon receiving a PREPARE message, a validator transitions to a PRECOMMIT phase and sends a PREPARE message to the leader. When the leader receives a quorum of PREPARE messages, it broadcasts a PRECOMMIT message.
- (COMMIT) A validator that receives a PRECOMMIT message transitions into a COMMIT phase and sends a PRECOMMIT message to the leader. When the leader receives a quorum of PRECOMMIT messages, it broadcasts a COMMIT message.
- (DECIDE) Upon receiving the COMMIT message, a validator transitions into a DECIDE phase and sends a COMMIT message to the leader. When the leader receives a quorum of COMMIT messages, it broadcasts a DECIDE message. A validator that receives a DECIDE message considers that as indicating consensus, adds the block to its blockchain, resets its timer and returns to the PREPARE phase for the next view.

Unlike IBFT, a timer expiry does not initiate a separate protocol for view change. Instead, the validator with the expired timer doubles its timer duration, transitions into the PREPARE phase for the next view, and sends a NEW-VIEW message (for the same block) to the leader for the next view.

3.2 Network Topology

Most BFT protocol designs are independent of the network topology connecting the nodes (where the validators are). In effect, the nodes are directly connected to each other via a *clique*. We consider this a virtual topology, as it is not scalable (consider the quadratic node-node links).

We are interested in how the underlying physical topology affects protocol performance. We therefore only consider those that can be unambiguously parameterized. Wide-area networks do not fit this requirement well. We therefore restrict our attention to BFT protocols that run within a single datacenter (e.g. enterprise blockchains). There are many possible datacenter network topologies. We pick two that have contrasting designs: Folded Clos [29] and Dragonfly [25].

3.2.1 Terminology and Notation (Topology).

A topology \mathcal{T} is a graph that connects *switches* with *links* as edges. Switches help to route messages between validators. The nodes that run validators, called *terminal nodes*, connect to this network via *edge switches*. The edge switch that has a leader connected to it is called the *leader switch*.

The Dragonfly is a *direct* network consisting of only edge switches (all have terminal nodes attached). The Folded Clos is an *indirect* network that has both edge and non-edge switches.

Let v_s be the number of switches and v_e the number of edge switches. Let $h_{\mathcal{T}}$ be the average hop distance in topology \mathcal{T} , i.e. the number of switches between a pair of validators.

We now describe the two topologies.

3.2.2 Folded-Clos.

We consider only a 3-level *Folded-Clos* indirect network with edge switches in level 1. To minimize the number of topology parameters, we assume each level has v_e switches, so $v_s = 3v_e$.

Let v_{12} be the number of links to level 2 switches from a level 1 edge switch. We require v_{12} to divide v_e , and the number of links to a level 3 switch from a level 2 switch is v_e/v_{12} .

Terminal nodes are connected to level 1 switches in a way that minimizes the maximum number of validators per edge switch (i.e. even distribution).

Fig. 3(a) and (b) illustrate the Folded-Clos($v_e = 8, v_{12} = 4$) and Folded-Clos($v_e = 9, v_{12} = 3$).

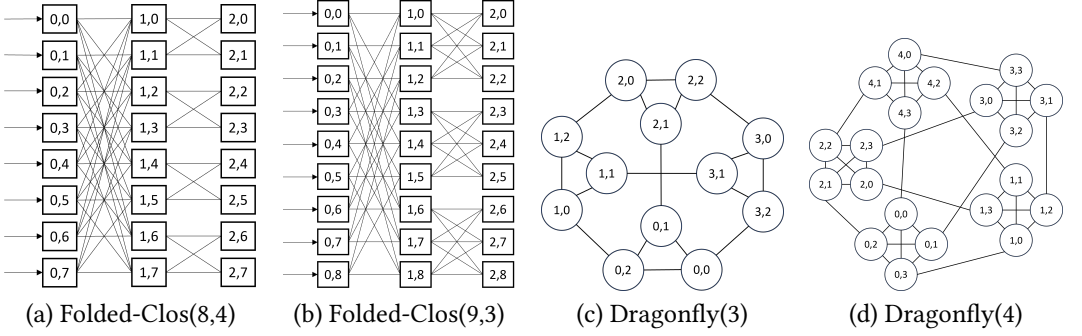


Fig. 3. Topology examples with parameters (a) $v_e = 8, v_{12} = 4$; (b) $v_e = 9, v_{12} = 3$; (c) $v_d = 3$; (d) $v_d = 4$.

3.2.3 Dragonfly.

In general, a Dragonfly is a direct network that divides switches into groups, with links between groups and possibly multiple intra-group topologies. Again, to minimize the number of topology parameters, we consider the following 1-parameter variant:

Let v_d be the number of switches connected by a clique in a group. Each switch in a group has a link to a switch in another group, so the number of groups is $v_g = v_d + 1$, and $v_s = v_g v_d = v_d(v_d + 1)$.

Like for the Folded-Clos, terminal nodes are evenly distributed over the switches.

Fig. 3(c) and (d) illustrate the topology for Dragonfly($v_d = 3$) and Dragonfly($v_d = 4$).

3.3 Performance

Fan et al. divide a distributed ledger architecture into 5 layers: application, execution, data, consensus and network [11]. We will focus on the performance of the consensus layer.

A user or administrator may be interested in the transaction latency or throughput. These are metrics for the data layer, where transactions arrive in a memory pool (mempool) and are grouped into blocks that are sent to the consensus layer [17]. Transaction latency therefore partly depends on the mempool protocol [9] above the consensus layer.

In steady state, the block throughput is determined by the transaction arrival rate in the data layer. We therefore focus on *block latency* ET , i.e. the average time between when a leader proposes a block and when consensus is reached. The “service rate” $1/ET$, together with the block throughput generated by the mempool protocol, determine the transaction latency. We therefore use a *closed* model to determine ET , i.e. every consensus generates another consensus instance.

Datacenters are multi-tenanted, so any blockchain must contend with network traffic from other workloads. Intuitively, running c blockchains concurrently should be equivalent to dividing switch rate by c , assuming the switches have little idle time. In the appendix, we present an experiment that confirms this intuition (see Fig. 12 in the Appendix). Therefore, the performance model will henceforth assume there is just 1 blockchain, with no competing network traffic. We first introduce some notation, before stating the equation that underlies the performance model.

3.3.1 Notation (Performance).

Let $T_{\mathcal{T}}^{\mathcal{P}}$ denote the consensus time for protocol \mathcal{P} and topology \mathcal{T} , where $\mathcal{P} = \mathcal{H}$ for HotStuff and \mathcal{I} for IBFT, and $\mathcal{T} = \mathcal{C}$ for clique, \mathcal{D} for Dragonfly and \mathcal{F} for Folded-Clos.

Let $r_v^{\mathcal{P}}$ and $r_s^{\mathcal{P}}$ be the rate for processing a protocol \mathcal{P} 's message at the validator and switch, respectively. (We assume the topology \mathcal{T} does not affect $r_v^{\mathcal{P}}$ and $r_s^{\mathcal{P}}$.) Let q denote the probability of a full round change when the leader is nonfaulty.

3.3.2 Consensus Time Model.

$ET_{\mathcal{T}}^{\mathcal{P}}$ depends critically on q . Round change scenarios can be complex, and can vary greatly with how \mathcal{P} handles timeouts. A full round change prompts a leadership change, and can be caused by a faulty leader, or timer expiry at non-leaders. We consider 3 possible events: \mathcal{E}_1 where the first leader for the consensus instance is faulty; \mathcal{E}_2 where the first leader is nonfaulty, but times out; and \mathcal{E}_3 where the first leader is nonfaulty and does not time out. Thus,

$$E(T_{\mathcal{T}}^{\mathcal{P}}) = E(T_{\mathcal{T}}^{\mathcal{P}}|\mathcal{E}_1)r + E(T_{\mathcal{T}}^{\mathcal{P}}|\mathcal{E}_2)(1-r)q + E(T_{\mathcal{T}}^{\mathcal{P}}|\mathcal{E}_3)(1-r)(1-q), \quad \text{where } r = n_f/n. \quad (1)$$

It remains to estimate $E(T_{\mathcal{T}}^{\mathcal{P}}|\mathcal{E}_j)$ for $j = 1, 2, 3$. Let $(T_{\mathcal{T}}^{\mathcal{P}})_3 = E(T_{\mathcal{T}}^{\mathcal{P}}|\mathcal{E}_3)$; this is the expected time if consensus finishes in 1 round (with no failures and timer expiry).

Throughout, we use “first-order approximations” that evaluate the most probable scenarios, and ignore less likely, complicated possibilities. In particular, we consider only a small number of faults.

3.4 Simulator

We use a simulator (see Fig. 11 in the appendix) to validate our performance model. Message service times at validators and switches are exponentially distributed by default, but these can be changed. Service rate $r_s^{\mathcal{P}}$ is relative to $r_v^{\mathcal{P}}$, and we set $r_v^{\mathcal{P}} = 1/3$ arbitrarily. Time unit for $T_{\mathcal{T}}^{\mathcal{P}}$ in all our plots follows that for $1/r_v^{\mathcal{P}}$. To factor out the impact of routing, the simulator uses ROMM routing [1], where a random next hop is chosen from alternative paths with minimal hop count.

We do just 1 simulation run per data point, so there are no confidence intervals for rigorously evaluating model accuracy. (The consensus time is averaged over 500–2000 consensus instances per run.) Our objective is to derive equations that provide performance insight, and we are ready to sacrifice numerical accuracy in exchange. The role of the simulator is more of a sanity check, to provide an assurance that the assumptions and approximations do not take the model far from the simulated reality, possibly making the extracted insights spurious.

4 CLIQUE TOPOLOGY

In this section, we factor out the topology by assuming the network is a clique. The results also apply for a non-clique with switches that are fast enough that inter-validator message delays are negligible. We divide the performance analysis into two cases: with/without full round change.

4.1 No Full Round Change

For now, assume initial timer value τ_0 is large and there are 0 faults. so there are no full round changes. Thus, $r = 0$ and $q = 0$, and $ET_{\mathcal{T}}^{\mathcal{P}} = E(T_{\mathcal{T}}^{\mathcal{P}}|\mathcal{E}_3)$ from Eqn.(1), so $ET_{\mathcal{T}}^{\mathcal{P}} = (T_{\mathcal{T}}^{\mathcal{P}})_3$.

For HotStuff, the leader is a performance bottleneck (see Fig. 2(b)). It has to process n votes (as leader) plus an additional message (as validator) for each of the first 3 phases. In the final phase, it need only process the first $n - f$ votes (before broadcasting DECIDE) plus one message (like any other validator). The total is $3(n + 1) + (n - f) + 1 = 4n - f + 4$. Thus,

$$\text{expected HotStuff consensus time is } (T_C^{\mathcal{H}})_3 = \frac{4n - f + 4}{r_v^{\mathcal{H}}} = \frac{11n + 13}{3r_v^{\mathcal{H}}} \quad \text{if } n = 3f + 1. \quad (2)$$

Note that this bottleneck analysis assumes the message queue is always nonempty, so there is no need for queueing theory [14].

For IBFT, all validators have to process 1 PRE-PREPARE, n PREPARE plus n COMMIT messages, so

$$\text{expected IBFT consensus time is } (T_C^{\mathcal{I}})_3 = \frac{2n + 1}{r_v^{\mathcal{I}}}. \quad (3)$$

Model Validation and Comparison (clique; no full round change)

The message processing times are random variables, so their arrival and departure times are random. Add to this the phase overlap among validators and between consecutive blocks, and it is not obvious that the above simplistic derivations would work. Nonetheless, we have validated Eqns. (2) and (3) with the simulator (the straightline plots are omitted here, in favor of other results).

HotStuff takes more phases to reach consensus than IBFT, but we can see clearly from Eqns. (2) and (3) that whether $(T_C^{\mathcal{H}})_3 > (T_C^{\mathcal{I}})_3$ depends on the relative values of $r_v^{\mathcal{H}}$ and $r_v^{\mathcal{I}}$. A similar comment applies if we compare how they scale with n , since $(T_C^{\mathcal{H}})_3 \approx \frac{11}{3r_v^{\mathcal{H}}}n$ and $(T_C^{\mathcal{I}})_3 \approx \frac{2}{r_v^{\mathcal{I}}}n$.

4.2 With Full Round Change

We can see from the simulation results in Fig. 1(a) that, if full round change can happen – because the timer value is too small or there are faults – then consensus time becomes non-monotonic.

4.2.1 HotStuff (clique; with full round change).

HotStuff has 4 phases, each with the leader broadcasting a message, and each validator processing it and replying with a vote. For the 4th phase, only $n - f$ votes are required before the leader broadcasts the DECIDE messages. The number of messages the leader needs to process is thus

$$m^{\mathcal{H}} = 3(n_w + 1) + n - f + 1 = 3(n - n_f + 1) + n - f + 1 = 4n - 3n_f - f + 4 \quad \text{so } (T_C^{\mathcal{H}})_3 = \frac{m^{\mathcal{H}}}{r_v^{\mathcal{H}}}. \quad (4)$$

A full round change occurs if the leader does not process $m^{\mathcal{H}}$ messages within τ_0 .

We now estimate $E(T_C^{\mathcal{H}}|\mathcal{E}_j)$ in Eqn. (1). For \mathcal{E}_1 , the first leader is faulty and the number of subsequent rounds is geometrically distributed. The timer has exponential backoff, and the final consensus round has time $(T_C^{\mathcal{H}})_3$, so $E(T_C^{\mathcal{H}}|\mathcal{E}_1) \approx \sum_{j=1}^{\infty} r^{j-1} (2^{j-1} \tau_0) + (T_C^{\mathcal{H}})_3 = (T_C^{\mathcal{H}})_3 + \frac{1}{1-2r} \tau_0$.

For \mathcal{E}_2 , the nonfaulty first leader times out. This is similar to having a faulty leader, so $E(T_C^{\mathcal{H}}|\mathcal{E}_2) = E(T_C^{\mathcal{H}}|\mathcal{E}_1)$. (We consider negligible the probability that both leaders of two consecutive rounds time out.) Thus Eqn.(1) gives

$$ET_C^{\mathcal{H}} = ((T_C^{\mathcal{H}})_3 + \frac{1}{1-2r} \tau_0)r + ((T_C^{\mathcal{H}})_3 + \frac{1}{1-2r} \tau_0)(1-r)q + (T_C^{\mathcal{H}})_3(1-r)(1-q) = (T_C^{\mathcal{H}})_3 + \frac{r + (1-r)q}{1-2r} \tau_0. \quad (5)$$

To estimate q , we consider the probability distribution for processing $m^{\mathcal{H}}$ messages. If the processing time X_i for the i th message has mean $\frac{1}{r_v^{\mathcal{H}}}$ and variance σ^2 , then we can use the Central Limit Theorem to approximate the processing time $Y = \sum_{i=1}^{m^{\mathcal{H}}} X_i \sim \mathcal{N}(m^{\mathcal{H}} \frac{1}{r_v^{\mathcal{H}}}, m^{\mathcal{H}} \sigma^2)$ and $q = \Pr(Y > \tau_0)$.

HotStuff Model Validation and Analysis (clique; with full round change)

Fig. 4 compares the model (Eqn. 5) to simulated consensus time for $n = 16$ and 32 , with full round change. It shows good agreement between model and simulator, except for small τ_0 , where the divergence is expected since “second-order effects” from complicated scenarios caused by a too-small τ_0 are no longer negligible.

We see from Eqn.(5) and the plot that, even when there are 0 faults ($r = 0$), $ET_C^{\mathcal{H}} = (T_C^{\mathcal{H}})_3 + q\tau_0$ increases from its minimum as τ_0 decreases on the left, raising timeout probability. If τ_0 is sufficiently large, so nonfaulty leaders do not timeout, then $q \approx 0$ and $ET_C^{\mathcal{H}} \approx (T_C^{\mathcal{H}})_3 + \frac{r}{1-2r} \tau_0$. Thus, the tail on the right in Fig. 4 is linear in τ_0 , and has gradient $\frac{r}{1-2r}$ that increases with number of faults n_f . Note that this effect depends on n_f and n only through the ratio $r = \frac{n_f}{n}$.

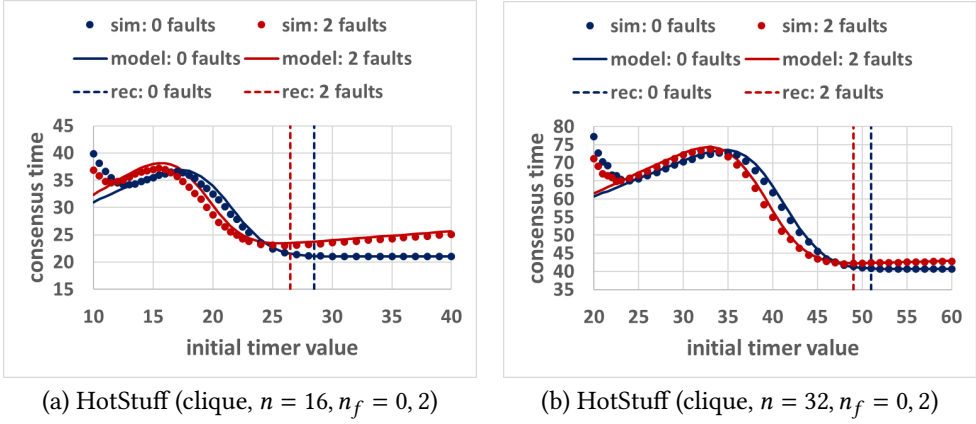


Fig. 4. Comparison of Eqn.(5) with simulation (with full round change). Vertical lines indicate τ_0^* (Eqn.(6)). The unit of time follows that for $1/r_v^P$ (see Sec. 3.4).

How should τ_0 be set? It should be larger than $(T_C^H)_3$, to provide some slack to accommodate the variance in T_C^H . One possibility is to give an allowance of 3 standard deviations, i.e.

$$\tau_0 \leftarrow \tau_0^* = m^H \frac{1}{r_v^H} + 3\sqrt{m^H} \sigma \quad \text{where } m^H = 4n - 3n_f - f + 4. \quad (6)$$

Note that r_v^H and σ can be measured with one-off profiling of message processing time.

Fig. 4 shows this recommended τ_0^* gives a good estimate of τ_0 where ET_C^H is minimum.

4.2.2 IBFT (clique; with full round change).

With n_f crash faults, Eqn.(3) becomes $(T_C^I)_3 = \frac{2n_w+1}{r_v^I}$. The specified order for leaders in IBFT makes it harder to derive closed-form expressions, so our model randomly chooses the leaders instead; this simplification should work well for large n . Thus, like HotStuff, the event \mathcal{E}_1 that i validators in a row are faulty leaders has probability $r^i = (\frac{n_f}{n})^i$, and $E(T_C^I | \mathcal{E}_1) \approx \sum_{j=1}^{\infty} r^{j-1} (2^{j-1} \tau_0) + (T_C^I)_3 + \frac{n_w}{r_v^I} = (T_C^I)_3 + \frac{1}{1-2r} \tau_0 + \frac{n_w}{r_v^I}$, since there are n_w round change messages. For \mathcal{E}_2 , the first leader times out like a faulty leader. There are possibly n_w excess messages from the penultimate round, and we estimate the final leader as processing $n_w(1-r)$ of them, after factoring out the crashed validators. Therefore, $E(T_C^I | \mathcal{E}_2) \approx E(T_C^I | \mathcal{E}_1) + \frac{n_w(1-r)}{r_v^I} = (T_C^I)_3 + \frac{1}{1-2r} \tau_0 + \frac{n_w(2-r)}{r_v^I}$ so Eqn.(1) gives

$$ET_C^I = (T_C^I)_3 + \frac{r + (1-r)q}{1-2r} \tau_0 + \frac{r + (2-r)(1-r)q}{r_v^I} n_w. \quad (7)$$

Compared to ET_C^H in Eqn.(5), the third term here is for round change messages.

For HotStuff, we estimate q by considering the messages a leader has to process before a timeout. In IBFT, however, everyone sends messages to everyone, and a validator decides once it receives a quorum of COMMIT messages. Thus, for a full round change to occur, more than f validators must undergo round change before they broadcast their COMMIT messages.

Simulations show that a full round change is usually caused by a leader who is delayed by a round change for the previous block. To model this event, suppose the full round change occurs for consensus instance i and, for consensus instance $i-2$, the n_w validators were synchronized at the start of their PREPARE phase. A validator will need to process $m^I = n_w + n - f$ messages to complete their PREPARE and COMMIT phases before the second timer in Fig. 2(a) expires.

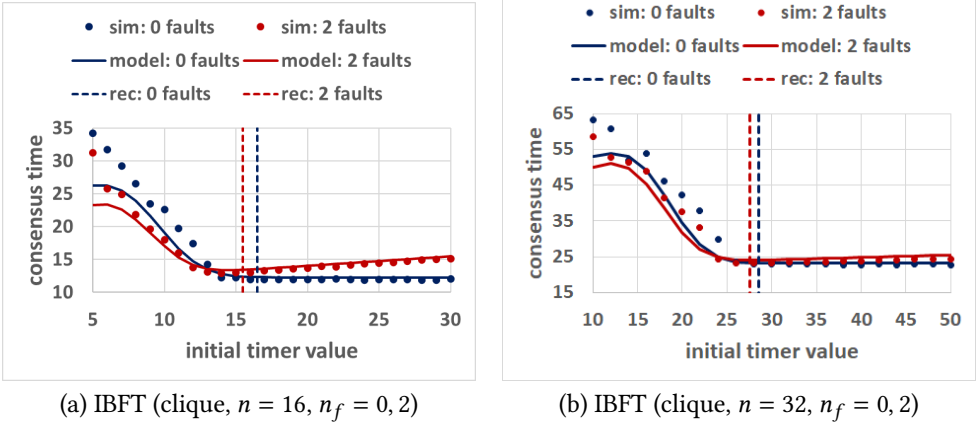


Fig. 5. Comparison of Eqn.(7) with simulation (with full round change). Leaders have a specified order in the simulation, but are randomly selected in the model. Vertical dashed lines indicate τ_0^* (Eqn.(8)).

Let $S_{i,k}$ be the time taken to process m^I messages by validator k in consensus instance i , and $X_k = S_{i-2,k} - \frac{1}{n_w} \sum_{j=1}^{n_w} S_{i-2,j}$. Then X_k measures how much faster or slower validator k is relative to the others at the end of instance $i-2$. Let σ^2 be the variance in message processing time. We then approximate the X_k distribution by $X_k \sim \mathcal{N}(0, m^I(1 + \frac{1}{n_w})\sigma^2)$.

When entering consensus instance $i-1$, faster validators (with $X_k < 0$) will enter the PREPARE phase $-X_k$ time earlier and wait for the m^I messages of slower validators. The consensus instance i round 1 leader, say validator c , is faster by $-X_c$, so the time it takes to process m^I messages is $Y = -X_c + S_{i-1,c} \sim \mathcal{N}(m^I \frac{1}{r_v}, m^I(2 + \frac{1}{n_w})\sigma^2)$ approximately, and we estimate $q \approx \Pr(Y > \tau_0)$ with this distribution.

IBFT Model Validation and Analysis (clique; with full round change)

Fig. 5 compares the IBFT model Eqn.(7) to simulated consensus time for $n = 16$ and $n = 32$. The agreement in the tail for large τ_0 is good, but diverges as τ_0 gets smaller. This is expected, since we needed multiple approximations to estimate q .

The tail (where $q \approx 0$) in Fig. 5 has the form $ET_C^I = (T_C^I)_3 + \frac{r}{1-2r}\tau_0 + \frac{r}{r_v}(n - n_f)$; for fixed n_f , this is still linear in τ_0 , with a gradient $\frac{r}{1-2r}$ (same as HotStuff) that increases with n_f and depends on n_f and n through r .

How should the timer be initialized? Using the same rule of thumb as before, it would be

$$\tau_0 \leftarrow \tau_0^* = m^I \frac{1}{r_v} + 3 \sqrt{m^I \left(2 + \frac{1}{n - n_f}\right) \sigma}, \quad \text{where } m^I = 2n - n_f - f. \quad (8)$$

Fig. 5 shows this τ_0^* gives a good estimation of where ET_C^I is minimum. Note that τ_0^* for IBFT is less sensitive to n and n_f for IBFT than for HotStuff ($2n - f$ vs $4n - f$ and $-n_f$ vs $-3n_f$).

5 NON-CLIQUE TOPOLOGY

Fig. 1(b) and (c) show that, for the Dragonfly, whether HotStuff is faster than IBFT depends on n and the switch rate. This is similarly true for Folded-Clos. In this section, we model how the topology impacts consensus time $ET_{\mathcal{F}}^P$. The approach is to focus on the validator and switch bottlenecks.

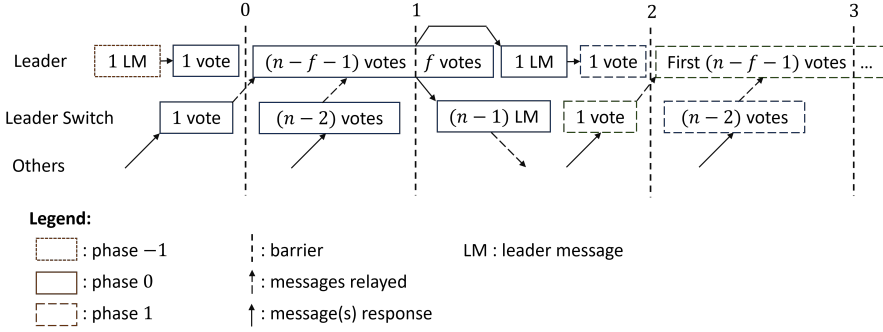


Fig. 6. Progress in HotStuff. Barrier0: leader ready to process phase 0 (PREPARE) votes from nonleaders. Barrier1: leader switch starts relaying leader's broadcast. Barrier2: leader ready to process phase 1 (PRECOMMIT) votes from nonleaders. PRECOMMIT, COMMIT and DECIDE phases have similar barriers.

5.1 No Full Round Change

As before, consider the case where τ_0 is large and validators are nonfaulty, so there is no full round change and $ET_{\mathcal{T}}^{\mathcal{P}} = (T_{\mathcal{T}}^{\mathcal{P}})_3$. Instead, we analyze the effect of changing n and switch rate $r_s^{\mathcal{P}}$.

5.1.1 HotStuff (non-clique; no full round change).

The HotStuff consensus time is mostly determined by the computation bottleneck at the leader and the communication bottleneck at the leader switch (where the leader is). Our analysis is based on the concept of *barriers* (see Fig. 6). For a specific round, we can take PREPARE to be phase 0, PRECOMMIT to be phase 1, etc. and DECIDE of the previous consensus instance to be phase -1.

Barrier0 marks the time after a leader processes the leader message for the previous consensus instance and its own vote; this is when the leader is ready to process phase 1 votes from nonleaders. Thus, the leader is guaranteed to have at least 1 of $n - f$ votes to process before the barrier.

Barrier1 marks the time after the leader has processed $n - f - 1$ additional votes and sent a broadcast, and the leader switch has cleared its queue (of $n - 2$ votes); this is when the leader switch is ready to relay the $n - 1$ broadcast messages.

Barrier2 marks the time after the leader switch has sent out the broadcast and relayed the first incoming vote to the leader ($n - 1 + 1$ messages), and the leader has processed all f remaining votes from phase 0, plus 1 vote and its own leader message; this is when the waiting pattern repeats and Barrier2 acts like Barrier0.

Similarly, Barrier3 is like Barrier1, etc. This pattern repeats up till the DECIDE phase, where there is only the portion between Barrier0 and Barrier1. After that, the remaining delay is for a validator to receive its DECIDE leader message to complete the consensus instance.

The time between Barrier0 and Barrier1 for each of HotStuff's 4 phases is $\max\{\frac{n-f-1}{r_v^{\mathcal{H}}}, \frac{n-2}{r_s^{\mathcal{H}}}\}$. The time between Barrier1 and Barrier2 for each of the 3 phases before DECIDE is $\max\{\frac{f+2}{r_v^{\mathcal{H}}}, \frac{n}{r_s^{\mathcal{H}}}\}$. It takes time $\frac{h_{\mathcal{T}}}{r_s^{\mathcal{H}}} + \frac{1}{r_v^{\mathcal{H}}}$ for a DECIDE message to reach a validator and be processed, and another $\frac{h_{\mathcal{T}}}{r_s^{\mathcal{H}}} + \frac{1}{r_v^{\mathcal{H}}}$ for the next leader to receive and process a NEW-VIEW message. Thus,

$$ET_{\mathcal{T}}^{\mathcal{H}} = (T_{\mathcal{T}}^{\mathcal{H}})_3 = 4 \max\left\{\frac{n-f-1}{r_v^{\mathcal{H}}}, \frac{n-2}{r_s^{\mathcal{H}}}\right\} + 3 \max\left\{\frac{f+2}{r_v^{\mathcal{H}}}, \frac{n}{r_s^{\mathcal{H}}}\right\} + 2\left(\frac{1}{r_v^{\mathcal{H}}} + \frac{h_{\mathcal{T}}}{r_s^{\mathcal{H}}}\right). \quad (9)$$

HotStuff Model Validation and Analysis (non-clique; no full round change)

Fig. 7 compares Eqn.(9) to simulated HotStuff consensus time for the Folded-Clos. (The Dragonfly

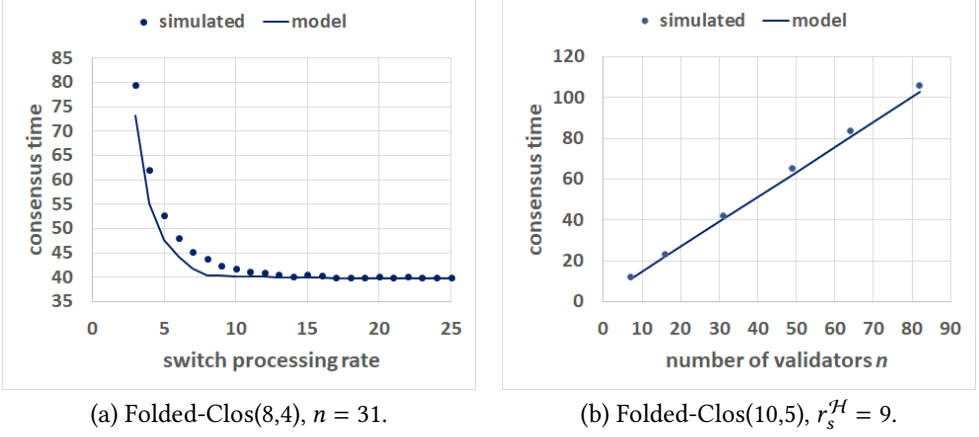


Fig. 7. Comparison of Eqn.(9) to HotStuff simulation (no full round change) for changes in (a) r_s^H and (b) n .

results are similar; this is not the case for IBFT.) In the Appendix, we show how the model's accuracy for Fig. 7(a) can be improved. Although that approximation is more accurate (see Fig. 13), extracting performance insight is harder, so we will continue with Eqn.(9).

We can tell from Eqn.(9) whether computation or communication dominates consensus time. Switching dominates the first max if $\frac{n-f-1}{r_v^H} < \frac{n-2}{r_s^H}$, i.e. $r_s^H < \frac{3f+1-2}{3f-f-1}r_v^H = \frac{3f-1}{2f}r_v^H$, and dominates the second max if $\frac{f+2}{r_v^H} < \frac{n}{r_s^H}$, i.e. $r_s^H < \frac{3f+1}{f+2}r_v^H$. Thus, HotStuff consensus time is mostly caused by network delays if $r_s^H < \frac{3}{2}r_v^H$ (independent of n). This can happen if switch rate r_s^H is reduced by cross traffic from other datacenter workloads (see Sec. 3.3 and Sec. A.0.1).

Note that topologies with $\frac{b_T}{r_s^H} \ll \frac{n}{r_s^H}$ would have similar HotStuff performance.

5.1.2 IBFT (non-clique; no full round change).

Every validator in IBFT has to broadcast messages, so the behavior is too complicated for a HotStuff-like leader-based barrier analysis. We therefore simplify the analysis further to just comparing the computation and communication bottlenecks, so $(T_{\mathcal{T}}^I)_3 \approx \max\{\frac{m_v}{r_v^I}, \frac{m_{\mathcal{T}}^I}{r_s^I}\}$, where the leader must process $m_v = 2n + 1$ messages (see Fig. 2(a)), and $m_{\mathcal{T}}^I$ is the number of messages the leader switch in topology \mathcal{T} must relay. There are 2 broadcasts and $(n - 1)$ PRE-PREPARE messages, so $m_{\mathcal{T}}^I = 2n_{\mathcal{T}}^I + (n - 1)$, where each broadcast requires relaying $n_{\mathcal{T}}^I$ messages.

For Folded-Clos, each validator sends and receives $(n - 1) + (n - 1)$ messages per broadcast. An edge switch has $k_{\mathcal{F}} (= \frac{n}{v_e})$ validators, so (after subtracting double-counting) it relays $n_{\mathcal{F}}^I = k_{\mathcal{F}}2(n - 1) - k_{\mathcal{F}}(k_{\mathcal{F}} - 1)$ messages.

For Dragonfly, a switch in any group G has a link to another switch in some other group G' , so it must relay $k_{\mathcal{D}}(v_d - 1)$ messages from the other validators in G to the $k_{\mathcal{D}}v_d$ validators in G' , and vice versa, for each of the broadcasts. Therefore,

$$ET_{\mathcal{T}}^I = (T_{\mathcal{T}}^I)_3 = \max \left\{ \frac{2n + 1}{r_v^I}, \frac{m_{\mathcal{T}}^I}{r_s^I} \right\}, \text{ where } m_{\mathcal{T}}^I = 2(k_{\mathcal{F}}2(n - 1) - k_{\mathcal{F}}(k_{\mathcal{F}} - 1)) + (n - 1), k_{\mathcal{F}} = \frac{3n}{v_s};$$

$$\text{and } m_{\mathcal{D}}^I = 2(k_{\mathcal{D}}2(n - 1) - k_{\mathcal{D}}(k_{\mathcal{D}} - 1)) + 2k_{\mathcal{D}}^2v_d(v_d - 1) + (n - 1), k_{\mathcal{D}} = \frac{n}{v_s}. \quad (10)$$

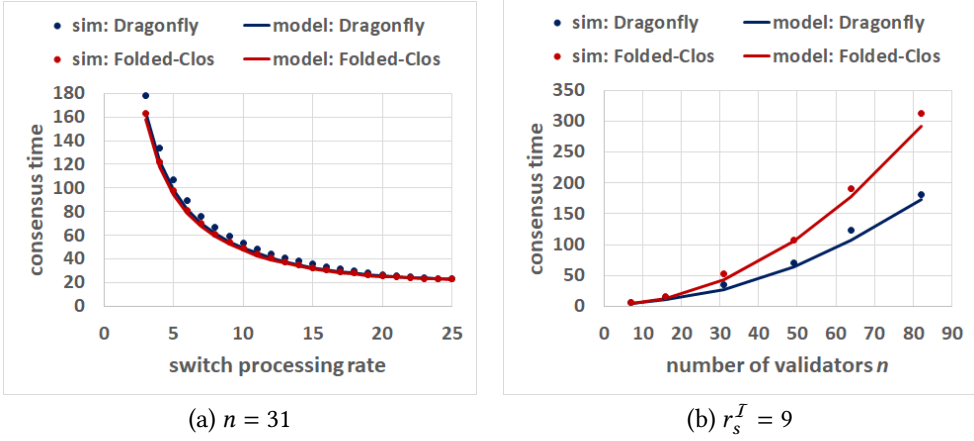


Fig. 8. Comparison of IBFT simulation (no full round change) to Eqn.(10) on Folded-Clos and Dragonfly for changing (a) switch rate r_s^I and (b) number of validators n .

IBFT Model Validation and Analysis (non-clique; no full round change)

Fig. 8 shows Eqns.(10) gives a good fit for simulated consensus times for both topologies. We now use the equations to compare HotStuff with IBFT, and Dragonfly with Folded-Clos.

HotStuff vs IBFT (non-clique; no full round change)

If r_s^P has greater impact than r_v^P , then we can simplify Eqn.(9) for HotStuff to $ET_{\mathcal{T}}^H = 4\frac{n-2}{r_s^H} + 3\frac{n}{r_s^H} + \frac{2h_{\mathcal{T}}}{r_s^H}$, which is linear in n . If the switches dominate IBFT performance, then Eqn.(10) gives $ET_{\mathcal{T}}^I = m_{\mathcal{T}}^I/r_s^I$ where $m_{\mathcal{T}}^I$ and $m_{\mathcal{D}}^I$ are quadratic in n . We can see this linear and quadratic behavior in Fig. 1(b).

However, suppose we fix $k_{\mathcal{T}}$ and scale the number of switches by $v_s = \frac{n}{k_{\mathcal{T}}}$. Then

$$ET_{\mathcal{F}}^I = \left(\frac{1}{r_s^I}\right)(6k_{\mathcal{F}}(2(n-1) - (3k_{\mathcal{F}} - 1)) + (n-1)) \text{ for Folded-Clos}$$

$$ET_{\mathcal{D}}^I = \left(\frac{1}{r_s^I}\right)\left(2k_{\mathcal{D}}(2(n-1) - (k_{\mathcal{D}} - 1) + 2n\frac{v_d(v_d-1)}{v_d(v_d+1)}) + (n-1)\right) \text{ for Dragonfly}$$

which are linear in n ($\frac{v_d(v_d-1)}{v_d(v_d+1)} \approx 1$ for large v_d).

Although IBFT consensus time is quadratic in n , Fig. 1(b) shows that IBFT can be faster than HotStuff for small n ; Fig. 1(c) shows a similar performance crossover point if the switch rate is sufficiently large. We can locate these crossover points by analyzing the closed-form expressions.

From Eqn.(9), $ET_{\mathcal{T}}^H = 4\frac{n-f-1}{r_v^H} + 3\frac{f+2}{r_v^H} + \frac{2}{r_v^H} = (4n-f+4)\frac{1}{r_v^H}$, while Eqn.(10) gives $ET_{\mathcal{T}}^I = m_{\mathcal{T}}^I/r_s^I$. The crossover $ET_{\mathcal{T}}^H = ET_{\mathcal{T}}^I$ occurs at

$$r_s^I = \frac{m_{\mathcal{T}}^I}{4n-f+4} r_v^H. \quad (11)$$

Fig. 9(a) compares Eqn.(11) to the simulated HotStuff/IBFT crossover points for the Dragonfly and Folded-Clos. The plot shows good agreement, despite many assumptions and approximations in the model.

One can do a similar analysis for a different choice of dominant terms in Eqns.(9) and (10).

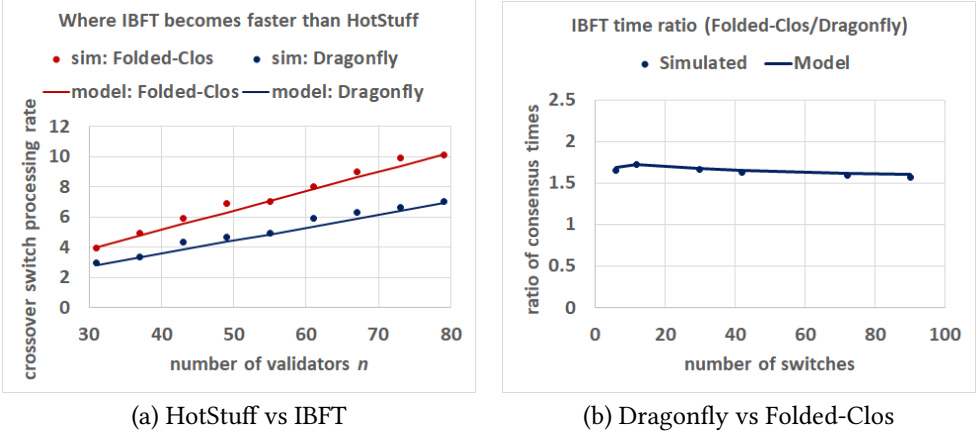


Fig. 9. Comparing simulation (no full round change) to (a) Eqn.(11) for switch processing rate r_s^I where IBFT becomes faster than HotStuff; (b) Eqn.(12) for IBFT consensus time ratio between Folded-Clos and Dragonfly for $k = 2$ (the simulated values are for $v_d(v_d + 1)$ divisible by 3).

Dragonfly vs Folded-Clos (IBFT; no full round change)

HotStuff's consensus times on Dragonfly and Folded-Clos are similar (see Eqn.(9)). This is also true for IBFT if computation time is the dominant factor, and the max in Eqn.(10) resolves to $\frac{2n+1}{r_o}$.

Consider now the case where IBFT performance is dominated by switching time. Suppose both topologies have the same number of switches v_s , $k_{\mathcal{F}} = \frac{n}{v_e} = \frac{3n}{v_s}$ and $k_{\mathcal{D}} = \frac{n}{v_e} = \frac{n}{v_s}$. Then

$$\frac{ET_{\mathcal{F}}^I}{ET_{\mathcal{D}}^I} = \frac{m_{\mathcal{F}}^I}{m_{\mathcal{D}}^I} = \frac{2k_{\mathcal{F}}(2(n-1) - (k_{\mathcal{F}} - 1)) + (n-1)}{2k_{\mathcal{D}}(2(n-1) - (k_{\mathcal{D}} - 1) + 2k_{\mathcal{D}}(v_d(v_d - 1))) + (n-1)} \approx \frac{1.5}{1 + \frac{1}{8k_{\mathcal{D}}}} \quad (12)$$

since $k_{\mathcal{D}}v_d(v_d - 1) = n \frac{v_d(v_d - 1)}{v_d(v_d + 1)}$ and $k_{\mathcal{F}} = 3k_{\mathcal{D}}$. Fig. 9(b) shows that, even for small v_d , $\frac{ET_{\mathcal{F}}^I}{ET_{\mathcal{D}}^I}$ is almost constant. The insight here is that, for the same number of switches, Folder-Clos is consistently slower than the Dragonfly (which spreads the n^2 communication workload over more switches).

5.2 With Full Round Change

5.2.1 HotStuff (non-clique; with full round change).

Here, we revisit the barrier analysis in Sec. 5.1.1. For Barrier1, the leader will still need to process $n - f$ messages to broadcast the message for the next phase. However, the leader switch will need to clear $n_w - 2$ votes before it starts relaying messages from the leader. The time required is thus $\max\{\frac{n-f-1}{r_v^{\mathcal{H}}}, \frac{n_w-2}{r_s^{\mathcal{H}}}\}$. Similarly, for Barrier2, the leader will still broadcast $n + 1$ messages, but will only have $f - n_f + 2$ messages (instead of $f + 2$) left to process since it received $n - n_f$ responses for that phase. Thus, with $n_f \neq 0$, Eqn.(9) becomes

$$ET_{\mathcal{F}}^{\mathcal{H}} = 4 \max\left\{\frac{n-f-1}{r_v^{\mathcal{H}}}, \frac{n-n_f-2}{r_s^{\mathcal{H}}}\right\} + 3 \max\left\{\frac{f-n_f+2}{r_v^{\mathcal{H}}}, \frac{n}{r_s^{\mathcal{H}}}\right\} + 2\left(\frac{1}{r_v^{\mathcal{H}}} + \frac{h_{\mathcal{F}}}{r_s^{\mathcal{H}}}\right) + \frac{r+(1-r)q}{1-2r}\tau_0. \quad (13)$$

(Note the impact of topology in $h_{\mathcal{F}}$ is the same as Eqn.(9).) We then estimate q as $\Pr(Y > \tau_0)$, where $Y \sim \mathcal{N}(\mu, \sigma^2)$, μ as in Eqn.(13) and

$$\sigma^2 = 4 \max\{(n-f-1)\sigma_v^2, (n-n_f-2)\sigma_s^2\} + 3 \max\{(n-n_f+2)\sigma_v^2, n\sigma_s^2\} + 2\sigma_v^2 + 2h_{\mathcal{F}}\sigma_s^2 \quad (14)$$

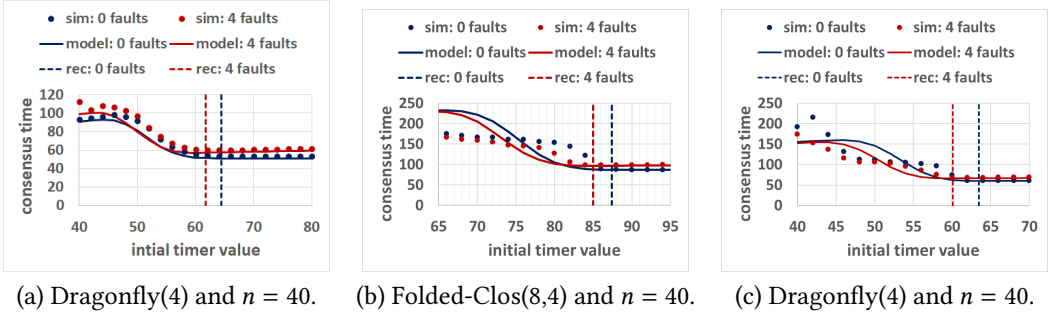


Fig. 10. Comparison of simulation to model for (a) HotStuff (similar for Dragonfly and Folded-Clos) using Eqns.(13) and (14), (b) IBFT Eqn.(15) for Folded-Clos and (c) IBFT Eqn.(15) for Dragonfly.

where σ_v and σ_s are standard deviations for validator and switch service times. Here, we use crude approximations $Var(X + Y) \approx VarX + VarY$ and $Var \max\{X, Y\} \approx \max\{VarX, VarY\}$.

5.2.2 IBFT (non-clique; with full round change).

For IBFT, we revisit the clique model in Sec. 4.2.2 for full round change. To factor in the topology, we consider the case where the switches are the bottleneck, so $(T_{\mathcal{F}}^I)_3 = \frac{m_{\mathcal{F}}^I}{r_s^I} = \frac{2n_{\mathcal{F}}^I + (n-1)}{r_s^I}$ from Eqn.(10). Each validator now sends $(n-1)$ messages and receives (n_w-1) messages per broadcast, so $n_{\mathcal{F}}^I = k_{\mathcal{F}}(n-1+n_w-1) - k_{\mathcal{F}}(k_{\mathcal{F}}-1)$ and $n_{\mathcal{D}}^I = k_{\mathcal{D}}(n-1+n_w-1) - k_{\mathcal{D}}(k_{\mathcal{D}}-1) + 2k_{\mathcal{D}}^2 v_d(v_d-1)(1-r)$ after factoring out crashed validators with $(1-r)$. The n_w messages in Eqn.(7) is now $n_{\mathcal{F}}^I$, so we get

$$ET_{\mathcal{F}}^I = \frac{2n_{\mathcal{F}}^I + (n-1)}{r_s^I} + \frac{r + (1-r)q}{1-2r} \tau_0 + \frac{r + (2-r)(1-r)q}{r_v^I} n_{\mathcal{F}}^I, \text{ where}$$

$$n_{\mathcal{F}}^I = k_{\mathcal{F}}(n + n_w - k_{\mathcal{F}} - 1) \text{ and } n_{\mathcal{D}}^I = k_{\mathcal{D}}(n + n_w - k - 1) + 2k_{\mathcal{D}}^2 v_d(v_d - 1)(1 - r). \quad (15)$$

Like for Eqn.(10), Eqn.(15) is quadratic in n for fixed v_s , but linear in n for fixed $k_{\mathcal{F}}$.

To estimate q in Eqns.(15), we combine the estimates in Sec. 4.2.2 (for full round change) and Sec. 5.1.2 (for non-clique). Per consensus instance, a validator only needs to process $m_v = m_{\mathcal{F}}^I - f + n_f - 1$ or $m_s = m_{\mathcal{F}}^I - k(f - n_f) - (n-1)$ messages (see Eqn.(10) for $m_{\mathcal{F}}^I$) in total before reaching consensus. The consensus time model is then $Y \sim \mathcal{N}(\max\{\frac{m_v}{r_v}, \frac{m_s}{r_s}\}, \max\{m_v(2 + \frac{1}{n_w})\sigma_v^2, m_s(2 + \frac{1}{n_w})\sigma_s^2\})$, where σ_v^2 and σ_s^2 are variances of message processing times at the validator and switch respectively. As before, we use 3 standard deviations for recommended τ_0^* .

Model with full round change for non-clique topology: Validation and Analysis

For HotStuff, Fig. 10(a) shows Eqn.(13) and the recommended τ_0^* fit the simulation reasonably well, despite the rough approximation in Eqn.(14) for q . Similar to the analysis of Eqn.(9), $ET_{\mathcal{F}}^{\mathcal{H}}$ is mostly caused by network delays if $r_s^{\mathcal{H}} < \frac{n-n_f-2}{n-f-1} r_v^{\mathcal{H}} = \frac{2f+(f-n_f)-1}{2f} r_v^{\mathcal{H}}$, so $n_f \neq 0$ lowers the threshold on $\frac{r_s^{\mathcal{H}}}{r_v^{\mathcal{H}}}$ from $\frac{3}{2}$ in Sec. 5.1.1 to 1.

For IBFT, however, Fig. 10(b) and (c) show Eqn.(15) does not fit the simulation well. Even so, the τ_0^* values are accurate, which indicate the model's location of the curve is on target.

We therefore extend Sec. 5.1's HotStuff vs IBFT analysis. Their comparison depends on q and r , so we only consider large τ_0 , where $q \approx 0$. Again, we focus on the case where the protocol's performance is determined by $r_v^{\mathcal{H}}$ and r_s^I . Then, Eqn.(13) and (15) give $ET_{\mathcal{F}}^{\mathcal{H}} = \frac{4(n-f-1)+3(f-n_f+2)+2}{r_v^{\mathcal{H}}} + \frac{r}{1-2r} \tau_0 =$

$\frac{4n-f-3n_f+4}{r_v^H} + \frac{r}{1-2r}\tau_0$ and $ET_{\mathcal{F}}^I = \frac{2n_s^I+(n-1)}{r_s^I} + \frac{r}{1-2r}\tau_0 + \frac{r}{r_s^I}n_{\mathcal{F}}^I$. (Note that, like for the clique in Sec. 4.2.1, the tails $\frac{r}{1-2r}\tau_0$ are the same.) Thus the crossover $ET_{\mathcal{F}}^H = ET_{\mathcal{F}}^I$ occurs at $r_s^I = \frac{(2+r)n_s^I+(n-1)}{4n-f-3n_f+4}r_v^H$, which generalizes Eqn.(11) for $n_f \neq 0$.

6 CONCLUSIONS

We conclude by highlighting some insights, derived from our analytical model on BFT consensus time, that are hard to obtain from simulations: how the initial timer value τ_0 should be set, and how it should scale differently with n for HotStuff and IBFT (Eqns.(6), (8)); how the two protocols have the same tail $\frac{r}{1-2r}\tau_0$, where r is the fraction of crash faults (Eqns.(13), (15)); how the bottleneck for HotStuff depends on r_s^H/r_v^H (Sec. 5.1.1, 5.2.1); how IBFT consensus time scales quadratically with n for fixed number of switches and linearly for fixed number of validators per edge switch (Eqns.(10), (15)); how the performance crossover between HotStuff and IBFT depends on r_s^I/r_v^H and scales with n (Eqn.(11), Fig. 9(a)); and how IBFT's consensus time ratio for Folded-Clos and Dragonfly is independent of n and number of switches (Eqn.(12), Fig. 9(b)). One can similarly draw more conclusions by considering a different choice of cases (in the max terms and bottlenecks).

We believe our modeling approach for IBFT can be used for analyzing other BFT protocols with similar message patterns, such as PBFT and BFT-SMART [4] (after including details like the reconfiguration protocol). It can also be combined with the approach for HotStuff to model a protocol like Zyzyva [15], which has a HotStuff-like message pattern for a "fast path" and a IBFT-like message pattern for a "slow path".

Similarly, our approach to analyzing the impact of the Dragonfly and the Folded-Clos should be applicable to other direct networks like the Slim-Fly [5] and indirect networks like the Hedera [2].

The analysis suggests some tips for analytical modeling that should apply to other consensus protocols: choose a metric that focuses on the protocol (Sec. 3.3); use the switch rate to factor out other network traffic (Sec. A.0.2); use bottleneck analysis instead of queueing theory (Sec. 4.1); use barrier analysis to mark the time when a node or switch changes phase (Fig. 6); do not shy away from crude approximations (e.g. using $\max\{EX, EY\}$ instead of $E \max\{X, Y\}$) that provide analytically tractable closed-form expressions — they may suffice to model the first-order effects and yield accurate conclusions (e.g. Fig. 9).

That said, it is clear that our modeling approach has reached its limit when modeling IBFT for non-clique topologies. Fig. 10(b) and (c) suggest that some other modeling element is necessary for q to shape the curve to fit the data.

REFERENCES

- [1] Dennis Abts and John Kim. 2011. *High Performance Datacenter Networks: Architectures, Algorithms, and Opportunities*. Morgan & Claypool Publishers. <https://doi.org/10.2200/S00341ED1V01Y2011103CAC014>
- [2] Mohammad Al-Fares, Sivasankar Radhakrishnan, Barath Raghavan, Nelson Huang, and Amin Vahdat. 2010. Hedera: Dynamic Flow Scheduling for Data Center Networks. In *Proceedings of the 7th USENIX Symposium on Networked Systems Design and Implementation, NSDI 2010, April 28-30, 2010, San Jose, CA, USA*. USENIX Association, 281–296. http://www.usenix.org/events/nsdi10/tech/full_papers/al-fares.pdf
- [3] Pierre-Louis Aublin, Rachid Guerraoui, Nikola Knezevic, Vivien Quéma, and Marko Vukolic. 2015. The Next 700 BFT Protocols. *ACM Trans. Comput. Syst.* 32, 4 (2015), 12:1–12:45. <https://doi.org/10.1145/2658994>
- [4] Alysson Neves Bessani, João Sousa, and Eduardo Adílio Pelinson Alchieri. 2014. State Machine Replication for the Masses with BFT-SMART. In *44th Annual IEEE/IFIP International Conference on Dependable Systems and Networks, DSN 2014, Atlanta, GA, USA, June 23-26, 2014*. IEEE Computer Society, 355–362. <https://doi.org/10.1109/DSN.2014.43>
- [5] Maciej Besta and Torsten Hoefler. 2014. Slim Fly: A Cost Effective Low-Diameter Network Topology. In *International Conference for High Performance Computing, Networking, Storage and Analysis, SC 2014, New Orleans, LA, USA, November 16-21, 2014*, Trish Damkroger and Jack J. Dongarra (Eds.). IEEE Computer Society, 348–359. <https://doi.org/10.1109/SC.2014.34>

- [6] Harold Carr, Christa Jenkins, Mark Moir, Victor Cacciari Miraldo, and Lisandra Silva. 2022. Towards Formal Verification of HotStuff-Based Byzantine Fault Tolerant Consensus in Agda. In *NASA Formal Methods - 14th International Symposium, NFM 2022, Pasadena, CA, USA, May 24-27, 2022, Proceedings (Lecture Notes in Computer Science, Vol. 13260)*, Jyotirmoy V. Deshmukh, Klaus Havelund, and Ivan Perez (Eds.). Springer, 616–635. https://doi.org/10.1007/978-3-031-06773-0_33
- [7] Miguel Castro and Barbara Liskov. 1999. Practical Byzantine Fault Tolerance. In *Proceedings of the Third USENIX Symposium on Operating Systems Design and Implementation (OSDI), New Orleans, Louisiana, USA, February 22-25, 1999*, Margo I. Seltzer and Paul J. Leach (Eds.). USENIX Association, 173–186. <https://dl.acm.org/citation.cfm?id=296824>
- [8] Allen Clement, Edmund L. Wong, Lorenzo Alvisi, Michael Dahlin, and Mirco Marchetti. 2009. Making Byzantine Fault Tolerant Systems Tolerate Byzantine Faults. In *Proceedings of the 6th USENIX Symposium on Networked Systems Design and Implementation, NSDI 2009, April 22-24, 2009, Boston, MA, USA*, Jennifer Rexford and Emin Gün Sirer (Eds.). USENIX Association, 153–168. http://www.usenix.org/events/nsdi09/tech/full_papers/clement/clement.pdf
- [9] George Danezis, Lefteris Kokoris-Kogias, Alberto Sonnino, and Alexander Spiegelman. 2022. Narwhal and Tusk: a DAG-based Mempool and Efficient BFT Consensus. In *EuroSys '22: Seventeenth European Conference on Computer Systems, Rennes, France, April 5 - 8, 2022*, Yérom-David Bromberg, Anne-Marie Kermerrec, and Christos Kozyrakis (Eds.). ACM, 34–50. <https://doi.org/10.1145/3492321.3519594>
- [10] Cynthia Dwork, Nancy A. Lynch, and Larry J. Stockmeyer. 1988. Consensus in the Presence of Partial Synchrony. *J. ACM* 35, 2 (1988), 288–323. <https://doi.org/10.1145/42282.42283>
- [11] Caixiang Fan, Sara Ghaemi, Hamzeh Khazaei, and Petr Musilek. 2020. Performance Evaluation of Blockchain Systems: A Systematic Survey. *IEEE Access* 8 (2020), 126927–126950. <https://doi.org/10.1109/ACCESS.2020.3006078>
- [12] Yossi Gilad, Rotem Hemo, Silvio Micali, Georgios Vlachos, and Nickolai Zeldovich. 2017. Algorand: Scaling Byzantine Agreements for Cryptocurrencies. In *Proceedings of the 26th Symposium on Operating Systems Principles, Shanghai, China, October 28-31, 2017*. ACM, 51–68. <https://doi.org/10.1145/3132747.3132757>
- [13] Suyash Gupta, Jelle Hellings, and Mohammad Sadoghi. 2021. RCC: Resilient Concurrent Consensus for High-Throughput Secure Transaction Processing. In *37th IEEE International Conference on Data Engineering, ICDE 2021, Chania, Greece, April 19-22, 2021*. IEEE, 1392–1403. <https://doi.org/10.1109/ICDE51399.2021.00124>
- [14] L. Kleinrock. 1974. *Queueing Systems, Volume I*. Wiley.
- [15] Ramakrishna Kotla, Lorenzo Alvisi, Michael Dahlin, Allen Clement, and Edmund L. Wong. 2009. Zyzzyva: Speculative Byzantine Fault Tolerance. *ACM Trans. Comput. Syst.* 27, 4 (2009), 7:1–7:39. <https://doi.org/10.1145/1658357.1658358>
- [16] Fan-Qi Ma, Quan-Lin Li, Yi-Han Liu, and Yan-Xia Chang. 2022. Stochastic Performance Modeling for Practical Byzantine Fault Tolerance Consensus in the Blockchain. *Peer-to-Peer Netw. Appl.* 15, 6 (2022), 2516–2528. <https://doi.org/10.1007/s12083-022-01380-x>
- [17] Dahlia Malkhi and Maofan Yin. 2023. Invited Paper: Lessons from HotStuff. In *Proceedings of the 5th Workshop on Advanced Tools, Programming Languages, and PLatforms for Implementing and Evaluating Algorithms for Distributed Systems, ApPLIED 2023, Orlando, FL, USA, 19 June 2023*, Yanhong Annie Liu and Elad Michael Schiller (Eds.). ACM, 3:1–3:8. <https://doi.org/10.1145/3584684.3597268>
- [18] Tianhui Meng, Yubin Zhao, Katinka Wolter, and Cheng-Zhong Xu. 2021. On Consortium Blockchain Consistency: A Queueing Network Model Approach. *IEEE Trans. Parallel Distributed Syst.* 32, 6 (2021), 1369–1382. <https://doi.org/10.1109/TPDS.2021.3049915>
- [19] Andrew Miller, Yu Xia, Kyle Croman, Elaine Shi, and Dawn Song. 2016. The Honey Badger of BFT Protocols. In *Proceedings of the 2016 ACM SIGSAC Conference on Computer and Communications Security, Vienna, Austria, October 24-28, 2016*, Edgar R. Weippl, Stefan Katzenbeisser, Christopher Kruegel, Andrew C. Myers, and Shai Halevi (Eds.). ACM, 31–42. <https://doi.org/10.1145/2976749.2978399>
- [20] Henrique Moniz. 2020. The Istanbul BFT Consensus Algorithm. *CoRR* abs/2002.03613 (2020). [arXiv:2002.03613](https://arxiv.org/abs/2002.03613) <https://arxiv.org/abs/2002.03613>
- [21] Saralees Nadarajah and Samuel Kotz. 2008. Exact Distribution of the Max/Min of Two Gaussian Random Variables. *IEEE Trans. Very Large Scale Integr. Syst.* 16, 2 (2008), 210–212. <https://doi.org/10.1109/TVLSI.2007.912191>
- [22] Qinyin Ni, Zhang Linfeng, Xiaorong Zhu, and Inayat Ali. 2022. A Novel Design Method of High Throughput Blockchain for 6G Networks: Performance Analysis and Optimization Model. *IEEE Internet Things J.* 9, 24 (2022), 25643–25659. <https://doi.org/10.1109/JIOT.2022.3194889>
- [23] Marshall C. Pease, Robert E. Shostak, and Leslie Lamport. 1980. Reaching Agreement in the Presence of Faults. *J. ACM* 27, 2 (1980), 228–234. <https://doi.org/10.1145/322186.322188>
- [24] Saulo Ricci, Eduardo Ferreira, Daniel Sadoc Menasché, Artur Ziviani, José Eduardo de Souza, and Alex Borges Vieira. 2018. Learning Blockchain Delays: A Queueing Theory Approach. *SIGMETRICS Perform. Evaluation Rev.* 46, 3 (2018), 122–125. <https://doi.org/10.1145/3308897.3308952>
- [25] Daniele De Sensi, Salvatore Di Girolamo, and Torsten Hoefler. 2019. Mitigating Network Noise on Dragonfly Networks Through Application-aware Routing. In *Proceedings of the International Conference for High Performance Computing, Networking, Storage and Analysis, SC 2019, Denver, Colorado, USA, November 17-19, 2019*, Michela Taufer, Pavan Balaji,

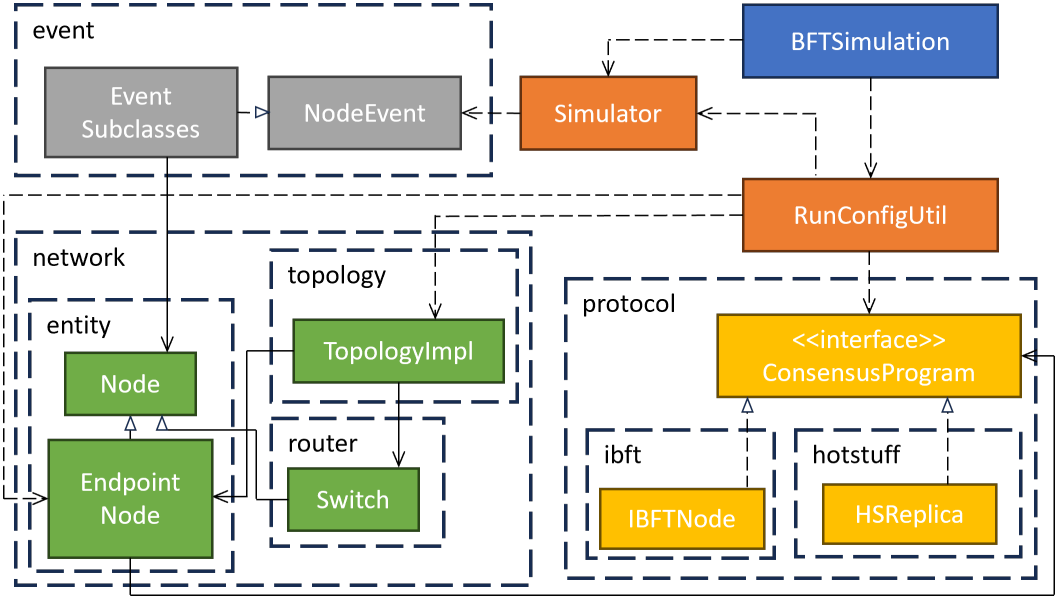


Fig. 11. Architecture diagram of the main components of the simulator program.

- and Antonio J. Peña (Eds.). ACM, 16:1–16:32. <https://doi.org/10.1145/3295500.3356196>
- [26] Chrysoula Stathakopoulou, Tudor David, Matej Pavlovic, and Marko Vukolic. 2022. [Solution] Mir-BFT: Scalable and Robust BFT for Decentralized Networks. *J. Syst. Res.* 2, 1 (2022). <https://doi.org/10.5070/sr32159278>
- [27] Y. C. Tay. 2018. *Analytical Performance Modeling for Computer Systems, Third Edition*. Morgan & Claypool Publishers. <https://doi.org/10.2200/S00859ED3V01Y201806CSL010>
- [28] Samuel Williams, Andrew Waterman, and David A. Patterson. 2009. Roofline: an Insightful Visual Performance Model for Multicore Architectures. *Commun. ACM* 52, 4 (2009), 65–76. <https://doi.org/10.1145/1498765.1498785>
- [29] Peter Willis, Miaoxin Li, and Nirmala Shenoy. 2023. Performance of Meshed Tree Protocol in Data Center Networks. In *Proceedings of the 2nd ACM SIGCOMM Workshop on Future of Internet Routing & Addressing, FIRA@SIGCOMM 2023, New York, NY, USA, 10 September 2023*. ACM, 15–22. <https://doi.org/10.1145/3607504.3609290>
- [30] Jie Xu, Cong Wang, and Xiaohua Jia. 2023. A Survey of Blockchain Consensus Protocols. *Comput. Surveys* 55, 13s (2023), 1–35.
- [31] Maofan Yin, Dahlia Malkhi, Michael K. Reiter, Guy Golan-Gueta, and Ittai Abraham. 2019. HotStuff: BFT Consensus with Linearity and Responsiveness. In *Proceedings of the 2019 ACM Symposium on Principles of Distributed Computing, PODC 2019, Toronto, ON, Canada, July 29 - August 2, 2019*, Peter Robinson and Faith Ellen (Eds.). ACM, 347–356. <https://doi.org/10.1145/3293611.3331591>
- [32] Pu Yuan, Kan Zheng, Xiong Xiong, Kuan Zhang, and Lei Lei. 2020. Performance Modeling and Analysis of a Hyperledger-based System Using GSPN. *Comput. Commun.* 153 (2020), 117–124. <https://doi.org/10.1016/J.COMCOM.2020.01.073>

A APPENDIX

For easy reference, Table 1 lists the frequently-used notation used in the paper.

The simulator we use for model validation is implemented in Java, with some 3000 lines of code. (The simulator is on GitHub and will be released with publication of this paper.) It has protocol and network packages that can facilitate implementation of different consensus protocols and network topologies. Fig 11 provides a high-level architecture diagram of the simulation program.

A.0.1 Competing network traffic.

We model background and cross traffic by reducing the switch rate r_s^P . To validate this approach, we run $c = 1, 2, 3$ chains concurrently in the simulator, without changing the switch processing

Table 1. Notation for parameters and variables.

protocol	\mathcal{P} τ_0 n n_w n_f r f	consensus protocol $\mathcal{P} = \mathcal{I}$ for IBFT, $\mathcal{P} = \mathcal{H}$ for HotStuff initial value for timer number of validators number of working (i.e. nonfaulty) validators number of faulty validators fraction of faulty validators, $r = \frac{n_f}{n}$ bound on n_f , $n_f \leq f$, $n = 3f + 1$
topology	\mathcal{T} v_s v_e v_{12} v_d v_g $k_{\mathcal{T}}$ $h_{\mathcal{T}}$	network topology $\mathcal{T} = \mathcal{C}$ (Clique) or \mathcal{D} (Dragonfly) or \mathcal{F} (Folded-Clos) number of switches number of edge switches, $v_e = \frac{v_s}{3}$ for Folded-Clos, $v_e = v_s$ for Dragonfly number of links to level 2 from a level 1 switch in Folded-Clos number of links from a Dragonfly switch number of groups in a Dragonfly, $v_g = v_d + 1$ number of validators per edge switch, $k_{\mathcal{T}} = \frac{n}{v_e}$ average number of network hops between two validators
performance	$T_{\mathcal{T}}^{\mathcal{P}}$ $r_v^{\mathcal{P}}$ $r_s^{\mathcal{P}}$ $m_{\mathcal{T}}^{\mathcal{P}}$ $n_{\mathcal{T}}^{\mathcal{P}}$ q \mathcal{E}_1 \mathcal{E}_2 \mathcal{E}_3 $(T_{\mathcal{T}}^{\mathcal{P}})_3$ $\mathcal{N}(\mu_*, \sigma_*^2)$	consensus time for protocol \mathcal{P} over topology \mathcal{T} service rate for a protocol \mathcal{P} message at a validator service rate for a protocol \mathcal{P} message at a switch number of \mathcal{P} messages a bottleneck switch in topology \mathcal{T} must process number of broadcast messages in $m_{\mathcal{T}}^{\mathcal{P}}$ q is probability $\Pr(\text{full round change} \mid \text{nonfaulty leader})$ event for faulty first leader event for nonfaulty first leader, but times out event for nonfaulty first leader, no timeout $E(T_{\mathcal{T}}^{\mathcal{P}} \mid \mathcal{E}_3)$ normal distribution with mean μ_* and variance σ_*^2

rate, but with validator processing rate increased by c (to model additional terminal nodes). On the other hand, the model has switch processing rate $r_s^{\mathcal{P}}/c$, and $r_v^{\mathcal{P}}$ unchanged.

Fig. 12 shows a good fit between this model and the simulation for IBFT on a Folded-Clos, confirming our intuition that we can model competing network traffic by having a single chain but a slower switch rate.

A.0.2 HotStuff (non-clique; no full round change; improved approximation).

Fig. 7(a) shows a significant difference between Eqn.(9) and simulated HotStuff consensus time. We now show one way of improving the accuracy.

Let $X_v^{\mathcal{H}}$ and $X_s^{\mathcal{H}}$ be random variables for message processing times at a validator and switch. Then Eqn.(9) can be written as

$$ET_{\mathcal{T}}^{\mathcal{H}} = 4 \max\{(n-f-1)EX_v^{\mathcal{H}}, (n-2)EX_s^{\mathcal{H}}\} + 3 \max\{(f+2)EX_v^{\mathcal{H}}, nEX_s^{\mathcal{H}}\} + 2EX_v^{\mathcal{H}} + 2h_{\mathcal{T}}EX_s^{\mathcal{H}}.$$

Now, $(n-f-1)EX_v^{\mathcal{H}} = EX$ where X is the sum of $n-f-1$ message processing times at a validator. Similarly, $(n-2)EX_s^{\mathcal{H}} = EY$ where Y is the sum of $n-2$ message processing times at a switch. Eqn.(9) thus uses $\max\{EX, EY\}$ to approximate $E \max\{X, Y\}$. Using the Central Limit Theorem, we have $X \sim \mathcal{N}((n-f-1)EX_v^{\mathcal{H}}, (n-f-1)VarX_v^{\mathcal{H}})$ and $Y \sim \mathcal{N}((n-2)EX_s^{\mathcal{H}}, (n-2)VarX_s^{\mathcal{H}})$.

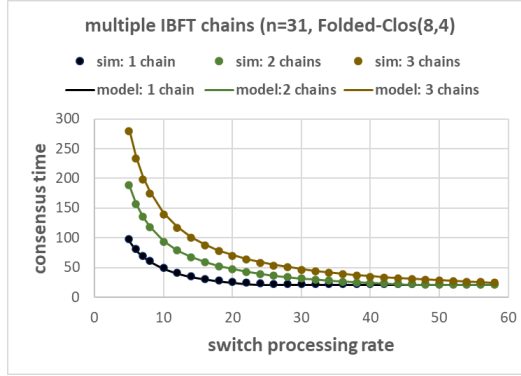


Fig. 12. Model with switch rate r_s^I/c fits consensus time for c simulated chains for IBFT on a Folded-Clos(8, 4) with switch rate r_s^I . The unit of time (on the vertical axis) follows that for $1/r_v^D$ (see Sec. 3.4).

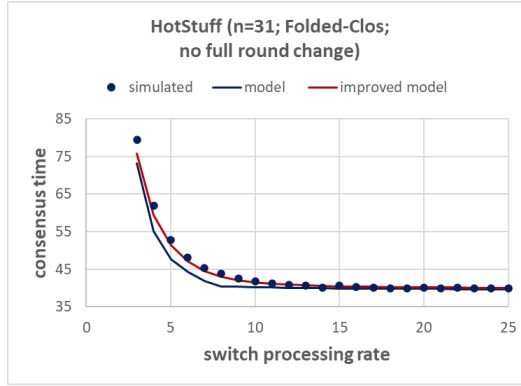


Fig. 13. Fig. 7(a) revisited: Comparison of simple model Eqn.(9) and improved model Eqn.(16) to simulation for HotStuff on Folded-Clos(8,4).

Therefore [21], $E \max\{X, Y\} \approx G(EX, VarX, EY, VarY)$ where

$$G(u_1, v_1, u_2, v_2) = u_1 \Phi \left(\frac{u_1 - u_2}{\sqrt{v_1 + v_2}} \right) + u_2 \Phi \left(\frac{u_2 - u_1}{\sqrt{v_1 + v_2}} \right) + \sqrt{v_1 + v_2} \phi \left(\frac{u_1 - u_2}{\sqrt{v_1 + v_2}} \right),$$

where ϕ and Φ are the standard normal density and cumulative distribution functions. We thus get the following alternative to Eqn.(9):

$$\begin{aligned} ET_{\mathcal{F}}^{\mathcal{H}} &= 4G\left((n-f-1)\frac{1}{r_v^{\mathcal{H}}}, (n-f-1)\sigma_v^2, (n-2)\frac{1}{r_s^{\mathcal{H}}}, (n-2)\sigma_s^2\right) \\ &\quad + 3G\left((f+2)\frac{1}{r_v^{\mathcal{H}}}, (f+2)\sigma_v^2, n\frac{1}{r_s^{\mathcal{H}}}, n\sigma_s^2\right) + \frac{2}{r_v^{\mathcal{H}}} + \frac{2h\tau}{r_s^{\mathcal{H}}} \end{aligned} \quad (16)$$

where $\sigma_v^2 = VarX_v^{\mathcal{H}}$ and $\sigma_s^2 = VarX_s^{\mathcal{H}}$.

Fig. 13 shows that Eqn.(16) gives a better approximation than Eqn.(9). However, this improved accuracy is at the expense of analytical tractability: one cannot use Eqn.(16) to compare HotStuff to IBFT, like we did with Eqn.(9) in Sec. 5.1.